Oxygen stoichiometry, crystal structure, and magnetism of $La_{0.5}Sr_{0.5}CoO_{3-\delta}$

2004 J. Phys.: Condens. Matter 16 6477

(http://iopscience.iop.org/0953-8984/16/36/013)

INSTITUTE OF PHYSICS PUBLISHING JOURNAL OF PHYSICS: CONDENSED MATTER

J. Phys.: Condens. Matter **16** (2004) 6477–6484 PII: S0953-8984(04)81216-5

Oxygen stoichiometry, crystal structure, and magnetism of $La_{0.5}Sr_{0.5}CoO_{3-\delta}$

Ryan P Haggerty[1] **and Ram Seshadri**[2,3]

[1] Department of Chemical Engineering, University of California, Santa Barbara, CA 93106, USA
[2] Materials Department and Materials Research Laboratory, University of California, Santa Barbara, CA 93106, USA

E-mail: hag@umail.ucsb.edu and seshadri@mrl.ucsb.edu

Received 25 May 2004
Published 27 August 2004
Online at stacks.iop.org/JPhysCM/16/6477
doi:10.1088/0953-8984/16/36/013

Abstract

We have prepared a series of polycrystalline samples $La_{0.5}Sr_{0.5}CoO_{3-\delta}$ with $0 < \delta \leqslant 0.21$ and characterized their oxygen content, crystal structure, and magnetic properties. While the fully oxygenated samples are good ferromagnets, samples with larger δ values display increasingly broad magnetic transitions. The saturation magnetization at 5 K falls rapidly as δ increases. First-principles electronic structure calculations provide insights into the magnetic behaviour of the fully oxygenated compound, and the manner in which ferromagnetic ordering is affected by increasing oxygen non-stoichiometry.

1. Introduction

$LaCoO_3$ has a rich history [1, 2] and yet remains the focus of a number of studies. For example, the temperature dependence of the structure of $LaCoO_3$ has been carefully re-examined by means of neutron [3] and single-crystal x-ray diffraction [4], with the latter providing evidence for orbital ordering at intermediate temperatures, as electrons are thermally activated from low- to intermediate-spin states.

The substituted, mixed-valence phases $La_{1-x}Sr_xCoO_{3-\delta}$ have also attracted a great deal of interest due to their finding use as cathodes in solid-oxide fuel cells [5–7], because they display colossal magnetoresistance [8, 9], and because they provide non-fatigue epitaxial electrodes for ferroelectrics [10]. In these compounds, it is well known that the crystal structure as well as the electrical transport and magnetic properties depend sensitively on the oxygen non-stoichiometry [11–14].

In this contribution, we have examined the effect of the oxygen non-stoichiometry δ on the properties of $La_{0.5}Sr_{0.5}CoO_{3-\delta}$. To our knowledge, this is the first systematic study describing

[3] http://www.mrl.ucsb.edu/~seshadri

how changes in δ influence structure and magnetic properties of $La_{0.5}Sr_{0.5}CoO_{3-\delta}$. A similar study of $La_{1-x}Sr_xCoO_{3-\delta}$ with $x = 0.0$ and 0.3 has been performed by Mineshige *et al* [13]. Sunstrom *et al* [12] have considered the effects of chemical oxidation of $La_{0.5}Sr_{0.5}CoO_{3-\delta}$. We have also considered the detailed electronic structure, from first-principles density functional calculations, of a plausible model for $La_{0.5}Sr_{0.5}CoO_{3-\delta}$ with $\delta = 0$: tetragonal $LaSrCo_2O_6$. Our calculations indicate that $La_{0.5}Sr_{0.5}CoO_{3-\delta}$ is a good ferromagnet, albeit with significant mixing of majority and minority states at the Fermi energy. It is such mixing that gives rise to a magnetic moment which is greatly reduced from the expected high-spin value.

2. Experimental details

La_2O_3 was dehydrated prior to use by firing at 900 °C for 24 h. $SrCO_3$, La_2O_3, and Co_3O_4 taken in appropriate stoichiometric amounts (a 0.01 mol basis) were ground together in an agate mortar and pestle, and heated in air at 850 °C for 24 h in a dense alumina crucible. The resulting powder was then reground, pelletized, and heated in air at 1100 °C for 24 h. A final reheating for 24 h, when required, was performed at 800 °C in different atmospheres.

For determining the oxygen content, redox titrations were performed by dissolving a weighed quantity (typically about 100 mg) of sample in 20 cm^3 of an acidified, 0.1 N Fe(II) sulfate solution. The ferrous ions reduce all cobalt to the Co(II) state. The amount of Fe(II) left over was determined by titration against a 0.1 N $K_2Cr_2O_7$ solution, with the end-point being determined electrochemically using a redox electrode. Three to five titrations were performed for each sample. Precise analysis of the titration data requires an accurate estimate of the mole numbers of the sample used. This in turn requires a knowledge of the oxygen content. A Mathematica™ Notebook was developed and used to perform this analysis in a self-consistent manner.

X-ray diffraction data were collected on a Scintag X-2 diffractometer operated in the Bragg–Brentano geometry and using Cu Kα radiation. Data were collected in the 2θ range of 10°–120° with a step size of 0.015° and a step time of 5 s. Rietveld refinement of the x-ray diffraction profiles made use of the XND Rietveld code [15]. Magnetization data as a function of temperature and field were collected using a Quantum Design MPMS 5XL magnetometer, operated between 5 and 350 K.

3. Computational methods

First-principles electronic structure calculations for $La_{0.5}Sr_{0.5}CoO_3$ were performed using the linear muffin tin orbital (LMTO) method within the atomic sphere approximation as implemented in the Stuttgart TB-LMTO-ASA program [16]. 396 k points in the irreducible wedge of the Brillouin zone were used for the calculation. The Perdew–Wang [17] formulation of the gradient-corrected exchange–correlation potential within the spin-density approximation was employed.

4. Results and discussion

Redox titrations indicate that the final heating atmospheres and/or protocols strongly control the oxygen non-stoichiometry δ in $La_{0.5}Sr_{0.5}CoO_{3-\delta}$, and δ can be tuned between 0.01 and 0.21. Table 1 lists the different atmospheres which allow these concentrations to be obtained. We henceforth refer to samples by their oxygen non-stoichiometry, δ. For the air-heated sample we obtain $\delta = 0.09(1)$, which is close to the value of $\delta = 0.06(1)$ reported by Señarís-Rodríguez

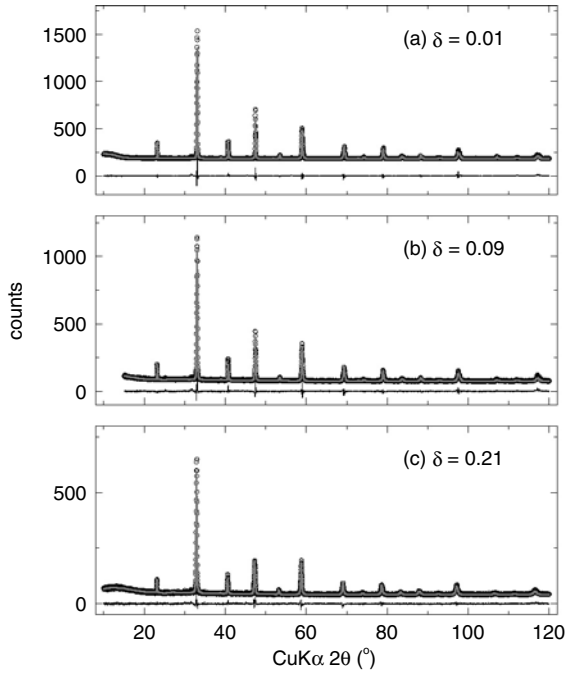

Figure 1. X-ray diffraction profiles (points), Rietveld fits, and difference profiles for $La_{0.5}Sr_{0.5}CoO_{3-\delta}$ with $\delta = 0.01$, 0.09, and 0.21. The data and fits have been slightly offset from the difference profile for clarity.

Table 1. List of the different annealing atmospheres (800 °C for 24 h) and the corresponding values of the oxygen non-stoichiometry δ in $La_{0.5}Sr_{0.5}CoO_{3-\delta}$ obtained from redox titration.

Atmosphere	δ	Error
O_2, slow cooling[a]	0.01	0.029
O_2	0.04	0.009
Air, as-prepared[b]	0.09	0.009
N_2	0.17	0.013
UHP Ar	0.21	0.022

[a] Cooled from 800 to 200 °C at 2 °C min^{-1}.
[b] This sample was not subjected to the final re-heating.

and Goodenough [11]. Sunstrom *et al* [12] obtain fully oxygenated $La_{0.5}Sr_{0.5}CoO_3$ in air, but from a slightly different heat treatment.

X-ray diffraction profiles (displayed for three samples in figure 1) of the different samples of $La_{0.5}Sr_{0.5}CoO_{3-\delta}$ are well fitted using the rhombohedral perovskite structure in a hexagonal setting ($R\overline{3}cH$). As δ increases, the widths of the Bragg peaks broaden and counts decrease indicating that microscopic inhomogeneities are created around the oxygen vacancies [7]. In keeping with the increased peak broadening and decreased counts, R_{Bragg} values systematically decrease from 9% for $\delta = 0.01$ to 7% for $\delta = 0.21$, broader profiles being easier to fit. When we used the cubic perovskite structure, the R_{Bragg} values were slightly higher for samples with small δ. As δ increases, peak broadening makes the rhombohedral distortion difficult to observe, and refinements in the cubic perovskite structure are equally satisfactory. Rhombohedral and cubic structures obtained from the refinements for different δ values are summarized in table 2.

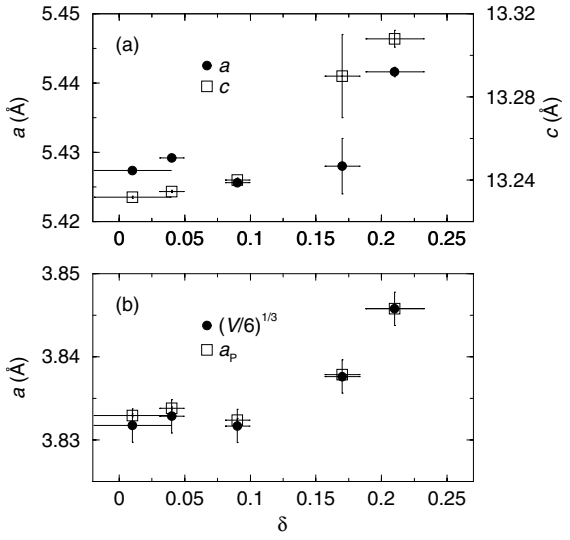

Figure 2. (a) Variation of the hexagonal a and c lattice parameters with δ. (b) Variation of the pseudocubic cell parameter calculated from the volume $[(V/6)^{1/3}]$ of the hexagonal cell with δ, compared with the δ dependence of the cubic perovskite cell parameter a_P obtained from Rietveld refinements using the cubic perovskite structure.

Table 2. Rhombohedral and cubic crystal structures obtained from the Rietveld refinements of the different $La_{0.5}Sr_{0.5}CoO_{3-\delta}$ samples.

	Rhombohedral[a], SG $= R\bar{3}cH$			Cubic[b], SG $= Pm\bar{3}m$
δ	a (Å)	c (Å)	x(O)	a_P (Å)
0.01	5.4274(2)	13.2317(6)	0.459(1)	3.8329(1)
0.04	5.4292(2)	13.2345(6)	0.459(1)	3.8337(2)
0.09	5.4256(3)	13.240(1)	0.456(2)	3.8324(2)
0.17	5.428(4)	13.29(2)	0.455(2)	3.8378(2)
0.21	5.4416(7)	13.308(4)	0.459(3)	3.8458(2)

[a] (La/Sr) at $(0, 0, \frac{1}{4})$; Co at (0, 0, 0) and O at $(x, 0, \frac{1}{4})$.
[b] (La/Sr) at $(\frac{1}{2}, \frac{1}{2}, \frac{1}{2})$; Co at (0, 0, 0), and O at $(\frac{1}{2}, 0, 0)$.

Figure 2 displays the variation of the hexagonal cell parameters a and c with δ. The initial increase in δ does not greatly influence the cell parameters. It is only when δ exceeds 0.1 that the cell parameters increase. This increase suggests why annealing experiments are limited as regards the range of δ which can be obtained, unlike the case for strained thin films (tensile strain on $SrTiO_3$, which has $a = 3.905$ Å) where much lower oxygen concentrations (larger δ values) have been reported [7].

To examine the effect of oxygen non-stoichiometry on the magnetic properties of $La_{0.5}Sr_{0.5}CoO_{3-\delta}$, we have recorded the temperature dependence of the magnetization for the different samples on warming in a 1000 Oe field, after cooling under zero field (ZFC), and on warming in a 1000 Oe field after cooling under a 1000 Oe field (FC). Data are displayed in figure 3(a). For δ smaller than 0.1, the samples show relatively sharp ferromagnetic transitions. The domain behaviour for this δ regime is typical of a hard ferromagnet. The $\delta = 0.17$ sample

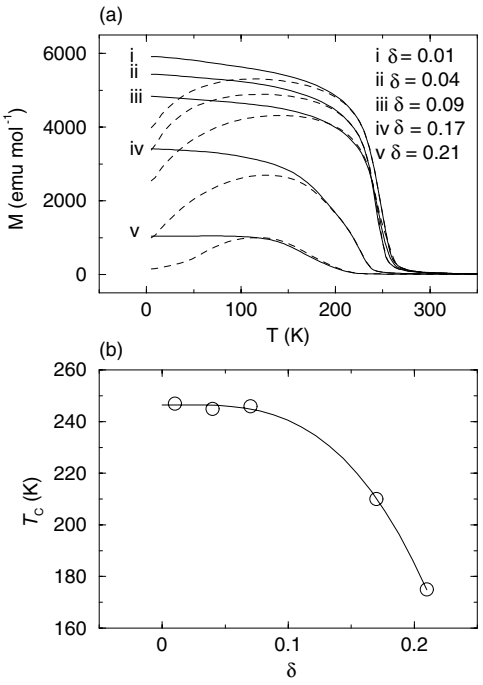

Figure 3. (a) ZFC (dashed) and FC (solid) magnetization of $La_{0.5}Sr_{0.5}CoO_{3-\delta}$ under a 1000 Oe field. (b) Variation of T_c with δ for $La_{0.5}Sr_{0.5}CoO_{3-\delta}$.

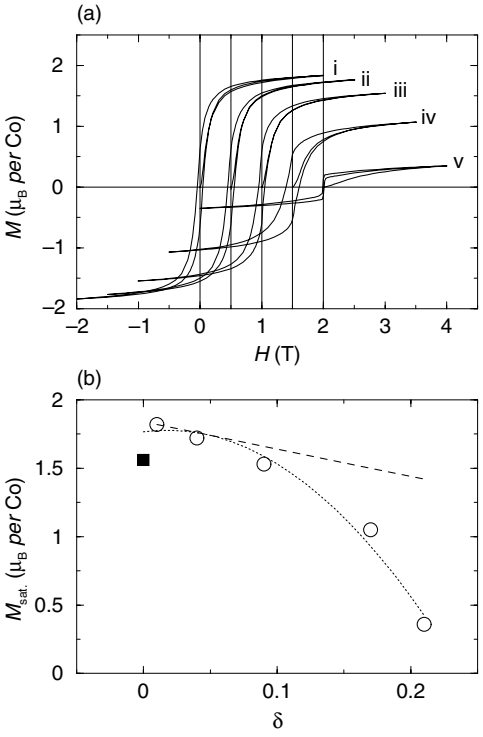

Figure 4. (a) Magnetization of $La_{0.5}Sr_{0.5}CoO_{3-\delta}$ with field at 5 K. The different labels (i)–(v) are the same as in the previous figure. The different loops have been shifted along the field axis for clarity. (b) Variation of M_{sat} (5 K, 2 T) with δ in $La_{0.5}Sr_{0.5}CoO_{3-\delta}$. The straight dashed line is the expected spin-only reduction of the saturation magnetization. The square is the magnetic moment from LMTO calculations.

has a rather broad transition. The $\delta = 0.21$ sample shows almost no ZFC magnetization at low temperatures. On warming, the magnetization displays a hump after a slow initial rise. To achieve further understanding of the origins of the unusual temperature dependence of the magnetization, we have carried out AC measurements under a 50 Oe field at frequencies of 10, 100, and 1000 Hz. We find no dispersion in the magnetization, or in the transition, ruling out the possibility of the presence of glassy magnetic phases. The variation in the Curie temperature with δ is displayed in figure 3(b). It is interesting that, paralleling the cell-parameter variation, there is hardly any change in T_c in the region $0 \leqslant \delta \leqslant 0.1$, but when $\delta \geqslant 0.1$, T_c drops rapidly. T_c for the oxygenated samples (near 250 K) is in agreement with earlier reports [12, 14].

Hysteresis loops of the 5 K magnetization of $La_{0.5}Sr_{0.5}CoO_{3-\delta}$ as a function of magnetic field are shown in figure 4(a). As δ increases the saturation magnetization is decreased. All the samples are hard magnets at 5 K. The coercive field increases with δ and then decreases, with a maximum corresponding to $\delta = 0.09$. The increased coercive field perhaps corresponds to structural imperfections which pin the magnetization. The sample with $\delta = 0.21$ shows unusual hysteretic behaviour. The initial rise from zero of the magnetization is rather slow, and is not retraced during the second field ramp. Once magnetized, the sample behaves like a soft ferromagnet.

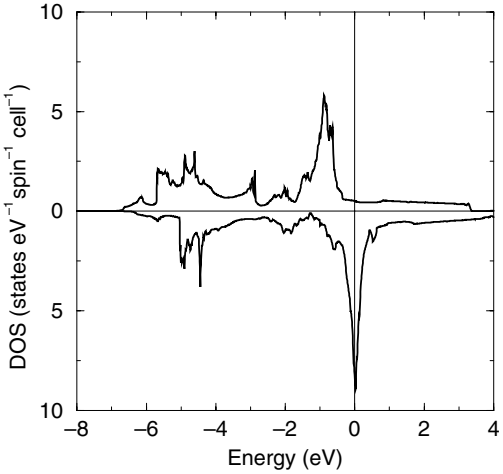

Figure 5. LMTO densities of states for tetragonal $LaSrCo_2O_6$ plotted in the two spin directions. The origin of the energy axis is the Fermi energy.

Figure 4(b) displays the variation of the 5 K saturation magnetization with δ. For $\delta = 0.01$, $M_{\text{sat}} = 1.82\ \mu_B$/Co. As δ increases, the saturation magnetization falls rapidly, following no simple trend. For example, if the decrease in Co oxidation state with increasing δ were translated into a simple reduction of the number of spins, the magnetization would be expected to fall according to $2 \times \delta$, indicated as a dashed curve, as discussed further in the section regarding the electronic structure. The actual fall is much larger than $2 \times \delta$. In figure 4(b), we have also displayed, as a filled square, the calculated (LMTO) magnetic moment for a sample that is effectively '$\delta = 0.00$'.

For density functional calculations, a model tetragonal ($P4/mmm$) structure was constructed by stacking a cubic perovskite ($a_P = 3.8329$ Å, directly obtained from Rietveld refinement in the cubic structure) cell of $LaCoO_3$ on top of a similar cubic perovskite cell of $SrCoO_3$. The effect of the artificial ordering of La and Sr has not been investigated; this is not expected to be significant because of the similarity in size. Of all $Ln_{0.5}A_{0.5}CoO_3$ phases, $La_{0.5}Sr_{0.5}CoO_3$ has the highest Curie temperature, in keeping with cation-size disorder being the least [14]. The pseudocubic perovskite of this composition is closely related in structure to the actual rhombohedral phase; indeed for the nearly fully oxygenated $\delta = 0.01$ sample, Rietveld refinement in the rhombohedral $R\overline{3}cH$ space group ($R_{\text{Bragg}} = 9.0\%$) was only a slight improvement over that in the cubic $Pm\overline{3}m$ space group ($R_{\text{Bragg}} = 11.6\%$). Taken together, we believe that these findings validate the model compound used for the calculation.

The calculations show how the saturation magnetization of $La_{0.5}Sr_{0.5}CoO_{3-\delta}$ is significantly reduced from the high-spin value, as a result of having both majority and minority spin states at the Fermi energy. The calculated magnetic moment, of 1.56 μ_B/Co atom, compared with experiment in figure 4(b), is slightly reduced from the experimental value of $M_{\text{sat}} = 1.82\ \mu_B$/Co obtained for the δ = 0.01 sample. It is in between the spin-only values for low-spin (LS) and high-spin (HS) octahedral $Co^{3.5+}$ in $La_{0.5}Sr_{0.5}CoO_3$, which are, respectively, 0.5 μ_B and 4.5 μ_B/Co. LMTO densities of states for tetragonal $LaSrCo_2O_6$ are displayed in figure 5 in the two spin directions. The origin of the energy axis is the Fermi energy. In the majority (↑) spin direction, the Fermi energy lies in a broad band just above a sharper, narrow band centred at around −1 eV and about 1.5 eV wide. In the minority (↓) spin direction, the same sharply peaked states are now centred at the Fermi energy. The

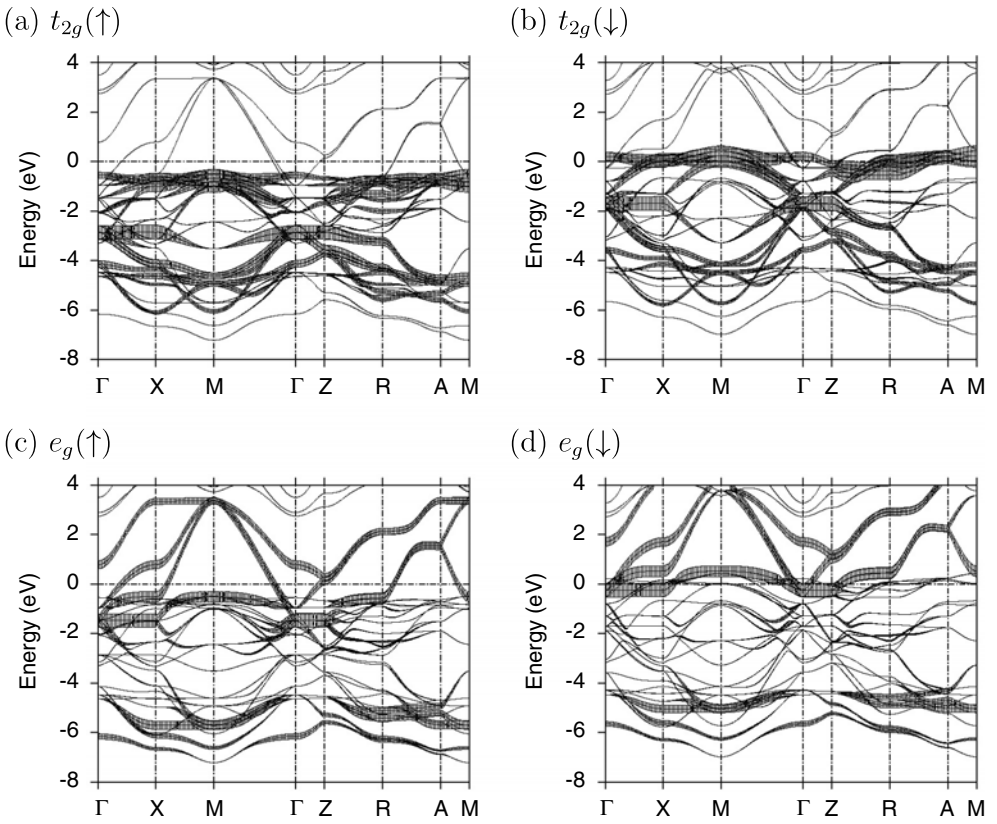

Figure 6. ((a), (c)) LMTO energy bands in the ↑ or majority spin direction and ((b), (d)) in the ↓ or minority spin direction. Bands deriving from Co t_{2g} and e_g states have been decorated as explained in the text.

exchange splitting is therefore the difference, which is 1 eV. It must be noted that such narrow, sharply peaked states at the Fermi energy would normally be suggestive of electron correlation, and an instability towards a Mott–Hubbard ground state. It is interesting that $La_{0.5}Sr_{0.5}CoO_3$ avoids such a ground state and remains a ferromagnetic metal, as is known from transport measurements [11], because of broader states which cross E_F in the majority spin direction.

A clearer understanding of the electronic structure is obtained from an examination of the band structures displayed in figures 6(a)–(d). A feature of the LMTO program is the ability to decorate bands with a width—so-called 'fatbands'—corresponding to specific orbital contributions to the different eigenvectors [18]. If, at some k point, the contribution from a specific orbital is 100%, then the width of the fatband at that point is 2.5% of the total energy scale, or in the present case, 0.3 eV.

The t_{2g} fatbands displayed in figures 6(a) and (b) in the two spin directions are not very disperse. In the ↑ band structure, t_{2g} states are centred at -1 eV. In the minority band structure (figure 6(b)), the widely dispersed t_{2g} states are centred around E_F with a width that is less than 2 eV. In figure 6(c), we observe that the partially filled $e_g(\uparrow)$ band is very disperse, extending in the Γ–M–X region of the Brillouin zone from approximately -1 to 3 eV. It is this band that gives rise to the disperse states which cross E_F in the majority spin direction, seen in figure 5. In the ↓ spin direction (figure 6(d)) it is seen that e_g states are empty, but similarly disperse.

It is well known for AMO_3 perovskites that corner-sharing of MO_6 octahedra results in those d states which point towards the ligand p orbitals, namely e_g states, being disperse because of M–O–M covalency, while the t_{2g} ones are narrow because d orbital lobes point away from ligand p. This is precisely what is observed in the electronic structure of $La_{0.5}Sr_{0.5}CoO_3$, which has bandwidths of approximately 1.5 and 4 eV for t_{2g} and e_g respectively.

The electronic structure of $La_{0.5}Sr_{0.5}CoO_3$ summarized in figures 5 and 6 emphasizes the danger in assigning spin states in extended solids. The e_g band is so much more disperse than t_{2g} that there is effectively no crystal field gap—this despite the centroids of the t_{2g} and e_g manifolds being separated by at least 3 eV. An exchange splitting of 1 eV in conjunction with a crystal field splitting of 3 eV would normally correspond to a low-spin configuration.

The electronic structure of $LaSrCo_2O_6$ allows us to speculate on the effect of creating oxygen vacancies. These would reduce the effective oxidation state of Co, resulting is a spin state which is close to low-spin, non-magnetic Co^{3+} with a t_{2g}^6 configuration. Increasing δ therefore concurrently reduces the number of unpaired spins as well as decreases the extent of spin polarization, accounting for the rapid fall in the saturation magnetization with δ observed in figure 4(b).

Acknowledgments

We thank Susanne Stemmer for suggestions and discussion. RH acknowledges support from the National Science Foundation through the RISE programme of the Materials Research Laboratory, and RS thanks the UCSB Academic Senate for a Junior Faculty Research Grant. This work made use of MRL facilities supported by the National Science Foundation under Award No DMR00-80034.

References

[1] Raccah P M and Goodenough J B 1967 *Phys. Rev.* **155** 932
[2] Bhide V G, Rajoria D S, Rama Rao G and Rao C N R 1972 *Phys. Rev.* B **6** 1021
[3] Radaelli P G and Cheong S W 2002 *Phys. Rev.* B **66** 094408
[4] Maris G, Ren Y, Zobel C, Lorenz T and Palstra T T M 2003 *Phys. Rev.* B **67** 224423
[5] Goodenough J B and Raccah R C 1963 *J. Appl. Phys.* **36** 1031
[6] Madhukar S, Aggarwal S, Dhote A M, Ramesh R, Krishnan A, Keeble D and Poindexter E 1997 *J. Appl. Phys.* **81** 3543
[7] Klenov D O, Donner W, Foran B and Stemmer S 2003 *Appl. Phys. Lett.* **82** 3427
[8] Mahendiran R, Mahesh R, Gundakaram R, Raychaudhuri A K and Rao C N R 1995 *J. Phys.: Condens. Matter* **7** L561
[9] Briceño G, Chang H Y, Sun X D, Schultz P G and Xiang X D 1995 *Science* **270** 273
[10] Cheng J T, Morgan P E D, Lowndnes D H, Zheng X-Y and Breen J 1993 *Appl. Phys. Lett.* **62** 2045
[11] Señarís-Rodríguez M A and Goodenough J B 1995 *J. Solid State Chem.* **118** 323
[12] Sunstrom J E, Ramanujachary K V and Greenblatt M 1998 *J. Solid State Chem.* **139** 388
[13] Mineshige A, Kobune M, Fujii S, Ogumi Z, Inaba M, Yao T and Kikuchi K 1999 *J. Solid State Chem.* **142** 374
[14] Vanitha P V, Arulraj A, Santhosh P N and Rao C N R 2000 *Chem. Mater.* **12** 1666
[15] Baldinozzi G, Bérar J-F and Calvarin G 1997 *J. Phys.: Condens. Matter* **9** 9731
[16] Jepsen O and Andersen O K 2000 *Stuttgart TB-LMTO-ASA Program* Version 47 (Stuttgart: MPI für Festkörperforschung)
[17] Perdew J P and Wang Y 1986 *Phys. Rev.* B **33** 8800
Perdew J P, Chevary J A, Vosko S H, Jackson K A, Pederson M R, Singh D J and Fiolhais C 1992 *Phys. Rev.* B **46** 6671
[18] Jepsen O and Andersen O K 1995 *Z. Phys.* B **97** 35